



Analysis of Chip Geometry in Hot Machining of Inconel 718 Alloy

Asit Kumar Parida¹

Received: 28 October 2016 / Accepted: 5 February 2018 / Published online: 28 February 2018
© Shiraz University 2018

Abstract

In the present work, the effect of heating temperature on the workpiece surface in orthogonal machining of Inconel 718 on chip geometry in terms of chip segmentation, shear band configuration, and equivalent chip thickness has been studied through scanning electron microscope of chip roots. Chip segment characteristics are an important phenomenon as it directly influences the cutting force during machining processes. The workpiece was heated with two heating temperatures of 300 and 600 °C by burning mixture of liquefied petroleum gas and oxygen. It was observed that with an increase in heating temperature equivalent chip thickness, the degree of segmentation, and serration frequency decrease compared to room-temperature machining conditions. It was also observed that shear plane length, shear band thickness decrease, whereas space between the shear band increases with the increase in heating temperature.

Keywords Hot machining · Chip segmentation · Inconel 718 · Adiabatic shear · Chip pitch · Chip frequency

1 Introduction

Inconel 718 alloys are widely used in aerospace, chemical, automobile, etc., machined components. The inherent properties which are responsible for the widespread use of Inconel 718 at high-temperature environment are also responsible for drastic tool wear during machining. The properties of Inconel 718 like low thermal conductivity, chemical reactivity, diffusivity, and high strength at high temperature are the properties which are unfavorable during machining. The temperature, pressure, and stress generated at cutting edge reduce the tool life, and hence rapid tool wear. Thermally enhanced machining process can overcome this problem and can improve machinability (Sun et al. 2010). In thermally enhanced machining process, an outer heating source was applied on the workpiece surface so that the shear strength of material reduces without affecting the metallurgical changes (Ezugwu et al. 2003). Different heating methods have been utilized by various researchers for enhancing machinability of high-strength materials. To improve machinability of Inconel

718, vast research has been carried out worldwide. Maity and Swain (2008) studied tool life using flame heating on manganese steel, and they found that tool wear decreased with the increase in heating temperature, and they developed a tool life equation and compared it with the experiment results. A good correlation between the predicted and measured tool life was noticed. Thandra and Choudhury (2010) presented tool life, surface finish, and cutting force using the gas flame heating method. They found that heating improves tool life and material removal rate, and reduces cutting force and surface roughness. Similarly, advanced technology like plasma and laser has been implemented for machining hard materials. Leshock et al. (2001) studied the numerical modeling of plasma-assisted machining of Inconel 718 and observed that cutting force reduced up to 30%, tool life increased 40%, and surface finish improved compared to the conventional machining process. The numerical results were validated with the experimental result, and good agreement was found. López de Lacalle et al. (2016) studied the machining of nickel base alloy using plasma as a heating source. They discussed influence of heating on tool wear and surface integrity of the machined surface. It was observed that the tool life and surface finish were better at plasma-assisted machining conditions compared to room-temperature conditions. Other researchers used different heating methods like laser (Norazlan et al. 2013; Germain et al. 2008),

✉ Asit Kumar Parida
asitzone4u@gmail.com

¹ Department of Mechanical Engineering, National Institute of Technology Rourkela, Rourkela, Odisha, India

plasma (Kittagawa and Maekawa 1990; Novak et al. 1997; Hinds and De Almeida 1981), flame heating (Maity and Swain 2008; Parida and Maity 2016a, b, c; Özler and Özel 2001), and induction heating (Baili et al. 2011; Ginta 2009; Ginta and Amin 2013) to study the machinability approach of high-strength material. These studies are related to the application of heating on tool wear, tool life, surface roughness, etc. But the study of chip morphology or chip segmentation lacks behind as per best knowledge in thermally enhanced machining process.

The control of segmentation of chip and shear band is the way to improve the machinability (Joshi et al. 2014). Machinability of Inconel 718 is poor because localization of heat in a narrow region in primary deformation zone causes rapid tool wear during machining which decreases the tool life and surface finish, and reduces material removal rate, etc. It was observed in the past study that shear localization is not possible due to less heat generation at low-cutting-speed condition. Heat-assisted machining process has some difficulties for studying the mechanism in terms of chip segmentation and the cyclic cutting force because of the complex and dynamic thermomechanical phenomenon. The effect of fracture criteria on chip segmentation was studied (Lorentzon et al. 2009). Two fracture criteria were studied, first, Cockroft–Latham model which is based on largest principal stress and effective plastic strain, and second, effective plastic strain. It was stated that thermal softening and material damage are the cause for changes of the continuous chip to segmentation chip, and effect of cutting speed is the most significant parameter for chip shape during machining. Other approaches like strain softening and thermal softening (Bäker 2005; Calamaz et al. 2008) were carried out for chip segmentation using finite element analysis. Chip serration frequency in machining of high-strength material is mostly affected by cutting speed compared to feed rate, and depth of cut was studied by Amin et al. (2012). The effect of chip morphology depends on the cutting parameters, contact friction, and thermomechanical loading (Komanduri and Brown 1981). Formation of chip segmentation of titanium alloy was studied (Hua and Shivpuri 2004; Cotterell and Byrne 2008). Effect of coolant pressure on tool wear in machining of two nickel base alloys (Inconel 718 and Waspaloy) was analyzed (Polvorosa et al. 2017), and it was shown that behaviors of both alloys are different in relation to pressure value. Certain speed ranges and cutting conditions are the two criteria for chip segmentation (Komanduri and Brown 1981). Self-excitation vibration, forced vibration, and dynamic response of the machine tool structure are other criteria for chip segmentation. The ratio between the inside and outside of the shear band within the chip was analysis chip segmentation is called segment intensity ratio (SIR). This is the effective way to find out

segmentation of chip compared to chip thickness, chip compression ratio for analysis of chip (Atlati et al. 2011). López de Lacalle et al. (2000) discussed the cutting conditions of machining of hard material like Ti–6Al–4V and Inconel 718. They discussed the effect of cutting speed, tooth feed, and helix angle on tool wear in machining of both materials. It was observed that both machinability problems were shown in the experiment. They concluded that machinability problem in titanium is due to low thermal conductivity and reactivity to the cutting tool, whereas machining problems in nickel were due to hardness and mechanical hardening. Parida and Maity (2016) discussed the effect of nose radius on cutting force and process parameters in hot machining of Inconel 718. They observed that the cutting force decreased at heating conditions compared to room-temperature conditions. In heating conditions, there was formation of continuous chips, whereas at room temperature, small chips or segment type chips were formed which was validated by using FEM simulation.

It was found that preheating reduces the shear strength and shear localization due to suppression of dynamic recrystallization which is a major reason for adiabatic shear band formation (Joshi et al. 2014). The aim of this paper is to investigate the effect of heating temperature on chip formation process or chip morphology in machining of Inconel 718 alloy.

2 Experiment Procedure

All cutting trials were carried out on a center lathe. During heating, the workpiece was rotated at slow speed so that uniform heating is possible. Gas flame (Oxyacetylene) was utilized for heating the workpiece. The temperature of the work surface was measured using thermocouple via the temperature indicator display unit. The flame handle was connected with an automatic controller. First, the desired heating temperature is set to the temperature display unit and the workpiece was heated to the desired temperature. As soon as the desired temperature is reached, the flame handle automatically comes back from the workpiece and goes toward the workpiece whenever the temperature decreases. The chemical and mechanical properties of Inconel 718 are shown in Table 1. The tool properties of cemented carbide were density $11,900 \text{ kg/m}^3$, Young's modulus 63 GPa, Poisson's ratio 0.26, yield limit 4250 MPa, thermal expansion 5.4×10^{-6} , specific heat 334 J/kg K, and thermal conductivity 100, respectively. The heating system along with orthogonal machining schematic diagram is shown in Fig. 1. A tube of 50 mm outer diameter and 47 mm inner diameter with a thickness of 1.5 mm was used as workpiece material.

Table 1 Mechanical and physical properties of Inconel 718 (Yilbas et al. 2010)

Density (kg/m ³)	8200
Latent heat of melting (J/kg)	250,000
Solidus Temperature (K)	1528
Liquidus Temperature (K)	1610
Specific heat capacity	600
Thermal conductivity (W/m k) at 1500 K	30
Poisson's ratio	0.3

The tool used for these experiments was triangular uncoated cemented carbide insert (TNGP). The machining experiments were carried out with three cutting speeds (40, 60 and 100 m/min), two heating temperatures (300 and 600 °C), and constant feed and depth of cut of 0.13 mm/rev, 1.5 mm, respectively. The chip shape and size were investigated with the help of optical and scanning electron microscope. The force was measured with the help of strain gauge dynamometer (SYSCON, INDIA).

3 Result and Discussion

Segmentation of chip and shear localization due to dry and hot machining has been explained in the result. Mechanism of chip formation, geometric parameters of a chip like segmentation ratio (SR), the frequency of serration, equivalent chip thickness, and its effect on cutting force were discussed in this section. Shear band spacing, shear

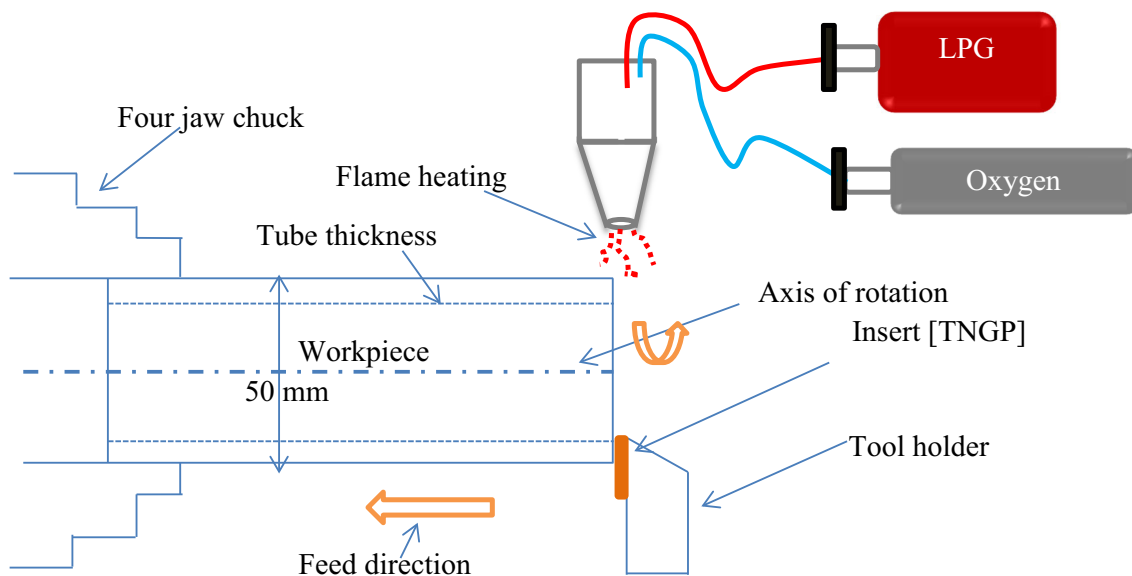
band thickness, and shear plane length were also analyzed at different heating and room temperature.

3.1 Influence of Heating on the Mechanism of Chip Formation

Different chip morphologies were obtained at different machining condition. At machining of 40 m/min cutting speed, there was no formation of segmental cutting chip, whereas as the cutting speed increased to 100 m/min, saw-tooth-type chip was observed as shown in Fig. 2a–c.

Inconel 718 is a low thermal conductivity material, and it is sensitive to strain hardening during machining. At room-temperature machining condition, the chip segments are formed by fracture and cover the entire chip as seen in Fig. 3a and its magnification view (b). The work hardening occurs due to higher strain rate work material deformation. But when heating temperature increases to 300 °C, thermal softening and fracture combination change the shape of the chip due to a decrease in strain rate sensitivity as shown in Fig. 3c and enlarged view (d).

When the optimum heating temperature was applied, i.e., 600 °C for Inconel 718, the fracture length decreased and only thermal softening occurred for segmentation of chip in Fig. 3e and its magnification view (f). Figure 4 shows the decrease in fracture length with an increase in heating temperature. The shape of segment chip was also affected by heating temperature. At room temperature, trapezoidal type of segment is formed due to plastic and shear deformation. In these conditions, all of the energy is not used in cutting process. But when machining

**Fig. 1** Schematic diagram of hot orthogonal machining setup

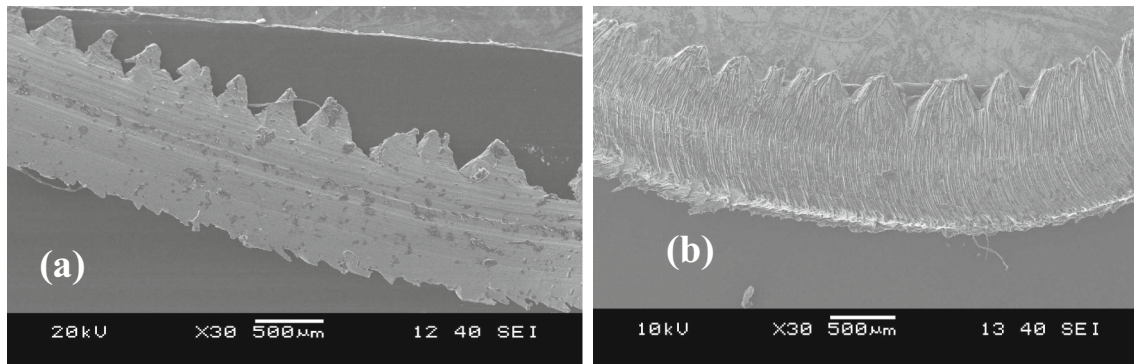


Fig. 2 Chip formation obtained at different machining environment **a** at 30 °C, **b** at 600 °C at cutting speed of 100 m/min

temperature increases, the chips forms a rectangular shape and the fracture length decrease 38%.

Similar observation was observed in preheating machining of Ti–6Al–4V alloy (Joshi et al. 2014) and milling of Ti–6Al–4V and Inconel 718 (López de Lacalle et al. 2000). It was observed that the fracture length in the chip root decreases with the increase in heating temperature. The moment of dislocation in the workpiece is restricted at low temperature, i.e., room temperature, and hence the formation of fracture occurs due to large strain induced in the shear plane during machining. But at high temperature, the material relieves the strain hardening because there is no restriction of the moment of dislocation, and hence fracture formation is reduced. At room temperature, the fracture length was measured and found 0.13 mm, but heating at 300 °C the fracture decreased to 0.13 mm, and again heating to 600 °C it comes to 0.11 mm. So 38% reduction in fracture occurs at 600 °C heating temperature. All measurements were noted on SEM image using the ImageJ software.

3.2 Analysis of Chip Segmentation or Chip Morphology at Different Machining Conditions

There are different parameters which affect the chip segment morphology, i.e., saw-tooth spacing, plastic strain, fracture, shear plane length, as shown in Fig. 5. Another two parameters which affect the chip morphology are affected by machining environment (segmentation ratio and frequency of serration).

3.2.1 Segmentation Ratio (SR)

The degree of segmentation ratio is the ratio between the differences of maximum chip thickness (H_{Max}) and minimum chip thickness (H_{Min}) to the maximum chip thickness (H_{Max}) as Eq. 1 is shown in Fig. 5.

$$\text{Segmentation ratio (SR)} = \frac{H_{\max} - H_{\min}}{H_{\max}}. \quad (1)$$

Due to the application of heating, the strength of material reduced compared to room-temperature machining. In heating conditions, plastic strain along the shear band increased and reduced maximum deformation segment H_{MAX} . At heating temperature, maximum deformation of material H_{MAX} decreased due to low strain rate sensitivity of work material. The segmentation ratio (SR) decreases 41, 40, and 56% at cutting speed 40, 60, and 100 m/min, respectively. But increasing cutting speed from 40 to 100 m/min, the segmentation ratio increased 65, 26, and 24% at 30, 300, and 600 °C heating temperature, respectively, as shown in Fig. 6.

3.2.2 Chip Segmentation Frequency (f_s)

Number of saw-tooth chip formed per second during the machining process. It can be calculated as Eq. 2 (Joshi et al. 2015)

$$\text{Segmentation frequency } (f_s) = \frac{\text{Cutting speed}}{\text{Undeformed Surface Length}}. \quad (2)$$

The frequency of chip segmentation decreased with the increase in heating temperature as shown in Fig. 7. The chip segmentation decreased 36, 13, and 11% at cutting speed of 40, 60, and 100 m/min, respectively, from room temperature to 600 °C heating temperature. This is due to undeformed chip length at room temperature which is less compared to 600 °C heating temperature. But when cutting speed increased from 40 to 100 m/min, the chip segmentation frequency increased 28, 51, and 78% at 30, 300, and 600 °C heating temperature. This may be due to plastic deformation at high strain rate and shear localization at high cutting speed.

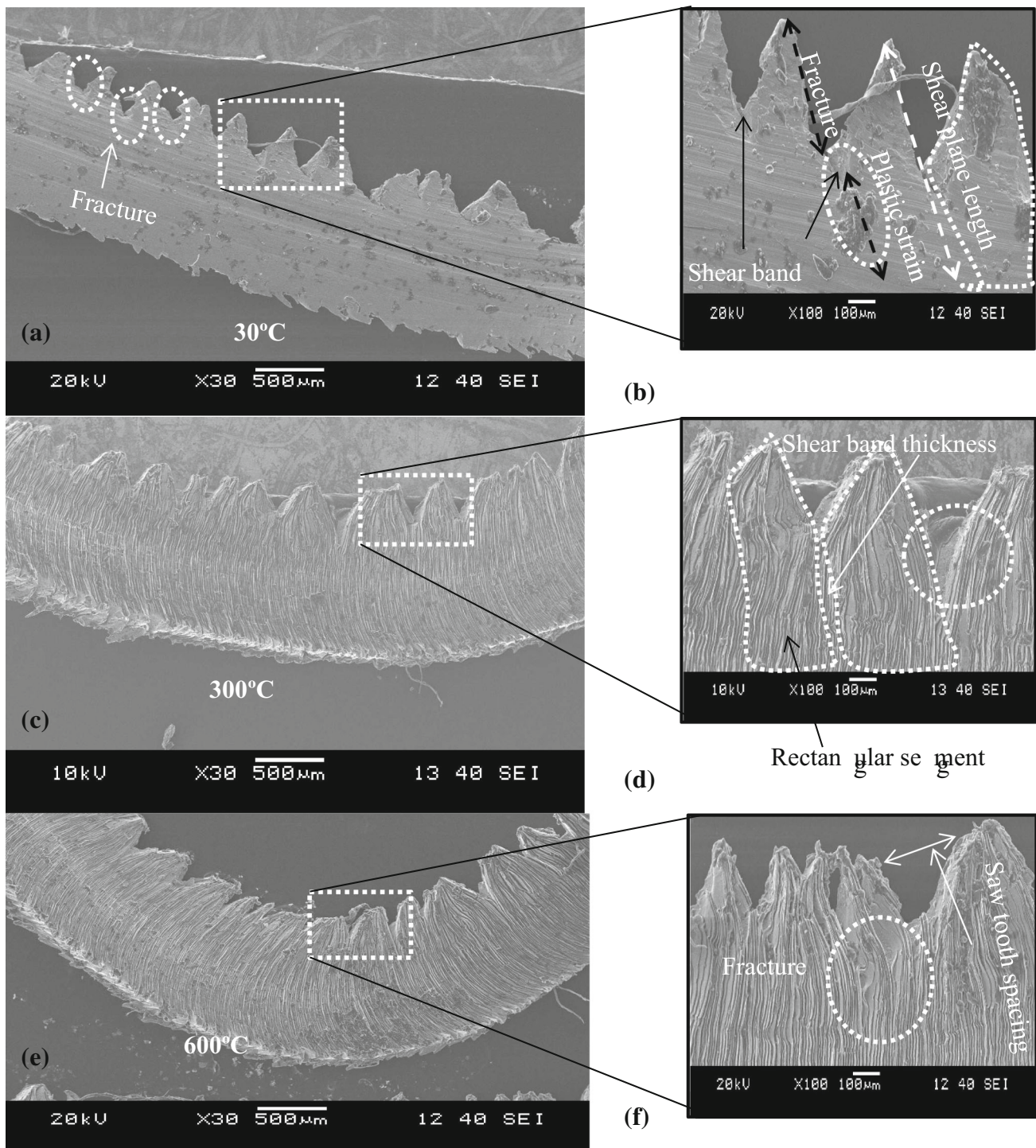


Fig. 3 Different chip segment taken in SEM at cutting speed of 100 m/min and feed rate of 0.13 mm/rev: **a** and **b** at room temperature **c** and **d** at 300 °C, **e** and **f** at 600 °C heating temperature

3.2.3 Equivalent Chip Thickness (H_{Eq})

Equivalent chip thickness in segmented chip can be calculated (Wang et al. 2014) in Eq. 3.

$$H_{Eq} = H_{max} + \frac{H_{max} - H_{min}}{2} \tag{3}$$

The formation of chip thickness in both room and the heating temperature is shown in Fig. 8. The equivalent chip

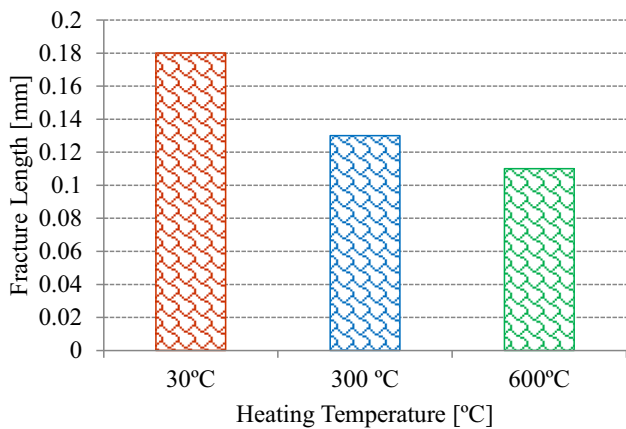


Fig. 4 Influence of fracture length on heating temperature at cutting speed 100 m/min

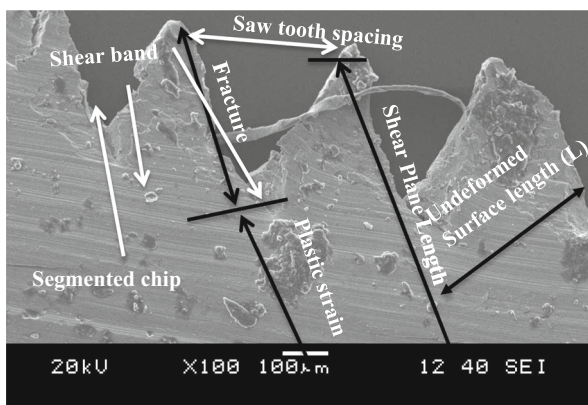


Fig. 5 Observation of mechanism of chip segmentation at cutting speed of 100 m/min at room temperature

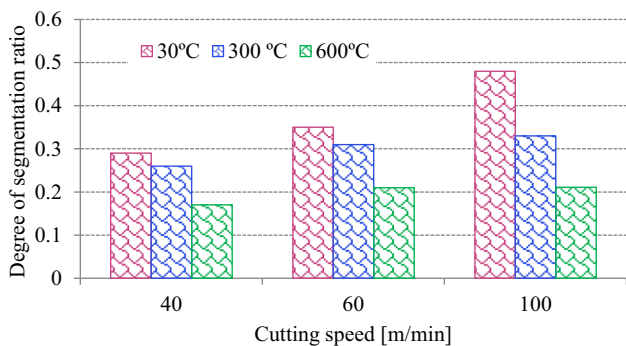


Fig. 6 Degree of segmentation ratio with respect to cutting speed at room and elevated temperature

thickness decreased with the increase in heating temperature.

There was an increase of 15, 28, and 23% of equivalent chip thickness at cutting speed 40, 60, and 100 m/min from room temperature to heating temperature of 600 °C. With the increase in cutting speed from 40 to 100 m/min, the

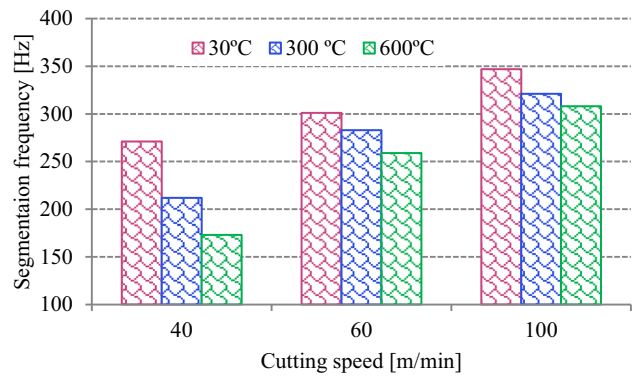


Fig. 7 Segmentation frequency versus cutting speed at different heating temperature

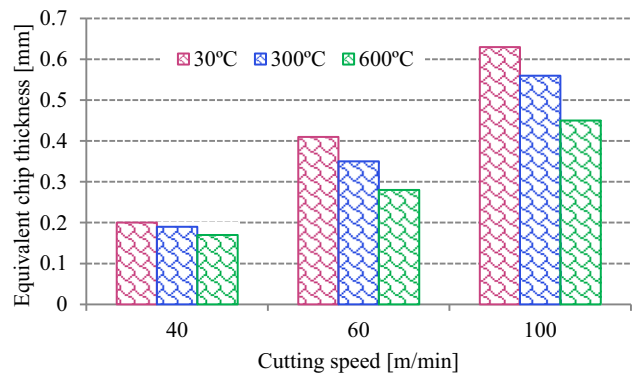


Fig. 8 Effect of heating temperature on equivalent chip thickness at different cutting speed

equivalent chip thickness increased 215, 194, and 164% at 30, 300 and 600 °C heating temperature, respectively.

3.2.4 Average Chip Pitch or Saw-Tooth Spacing (C_p)

It was observed that the average chip pitch decreased with the increase in heating temperature as shown in Fig. 9. There was a decrease of 21, 20, and 15% of average chip

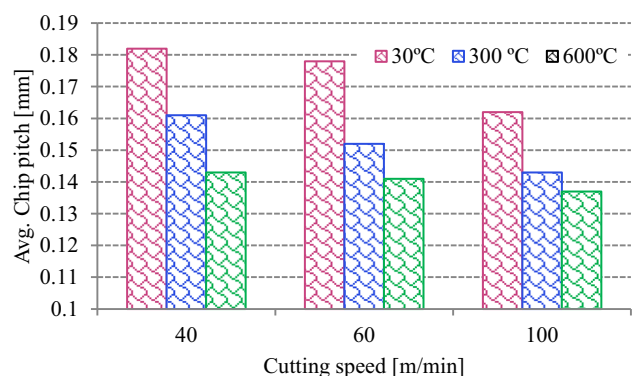


Fig. 9 Average chip pitch versus cutting speed at different heating temperature

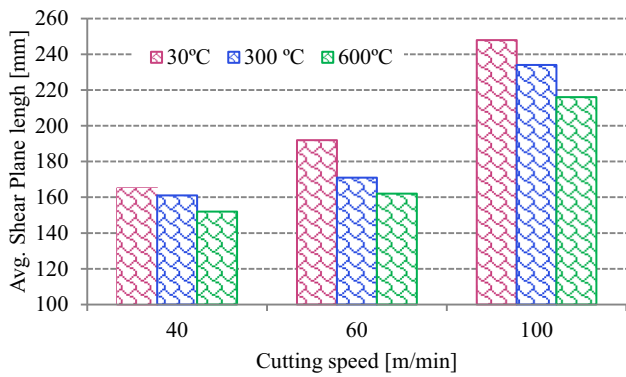


Fig. 10 Influence of heating temperature on average chip pitch and shear plane length at different cutting speed

pitch at cutting speed 40, 60, and 100 m/min, respectively, from room temperature to 600 °C heating temperature.

But with the increase in cutting speed from 40 to 100 m/min the average chip pitch decreased again 10, 11, and 4% at 30, 300 and 600 °C heating temperature, respectively. Similar observation was also found on thermally enhanced machining of Ti-6Al-4V (Joshi et al. 2014).

3.2.5 Average Shear Plane Length

Shear plane length indicates the maximum length of deformation a material undergoes while forming a segment. Material strength and heat generation during machining is also dependent on this parameter (Joshi et al.

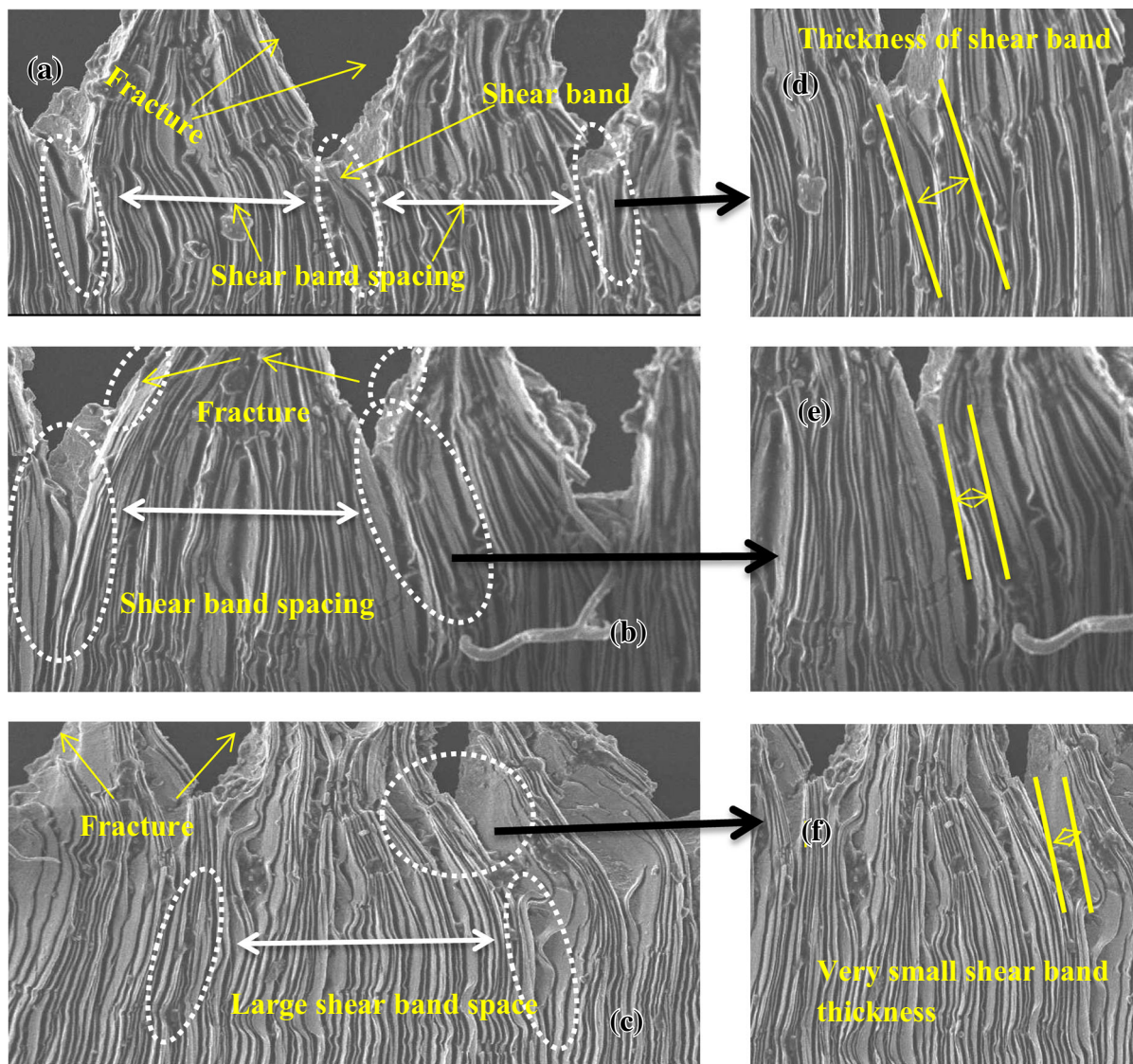


Fig. 11 Chip microstructure with different heating temperature (a–c) and their corresponding magnification image (d–f) at cutting speed of 100 m/min and feed of 0.13 mm/rev

2015). With the increase in heating temperature the average shear plane length decreased. The decrease in average shear plane length was 7, 15, and 12% at cutting speed 40, 60, and 100 m/min, respectively, from room temperature to heating temperature of 600 °C. This is because at high temperature heat generated due to plastic deformation decreases and lowers the material strength which is responsible for the increase in shear band spacing and segment pitch. But the average shear plane length increased 50, 45, and 42% with the increase in cutting speed from 40 to 100 m/min at 30, 300, and 600 °C heating temperature, respectively, as shown in Fig. 10.

3.3 Shear Band Configuration in Chip Due to Heating

Influence of shear band configuration was studied at room and different heating temperatures. Chip structure and shear band configuration at room and heating condition are shown in Fig. 11.

Again it was noticed that heating reduces the shear band thickness. This is due to suppression of dynamic recrystallization and increase in dynamic recovery during machining process as shear band formation involves the mechanism of rotational dynamic recrystallization (Xue et al. 2002). There was 66% (from 0.009 to 0.003 mm) reduction in the shear band from room temperature to 600 °C heating temperature as shown in Fig. 12a. Different types of assisted machining of hard material were also done by López de Lacalle et al. 2016.

Furthermore, the shear band spacing was also affected by heating temperature as shown in Fig. 12b. It was found that there was a 40% (from 108 μm to 152 μm) increase in spacing between the shear band from room temperature to 600 °C heating temperature. But at a heating temperature of 600 °C, segments are attached to a large part of the shear plane length. It concludes that contribution of plastic strain compared to fracture is high in segment formation and forms a more continuous type of chip.

3.3.1 Effect of Heating Temperature on Cutting Force

It was observed that the cutting force decreased with the increase in heating temperature. The reduction in cutting force 14, 15, and 11% at 40, 60, and 100 m/min cutting speed at a heating temperature of 600 °C was observed compared to room-temperature machining. This is due to the reduction in shear strength of the material due to heating of the workpiece. When cutting speed increased from 40 to 100 m/min, the cutting force again decreased 47, 50, and 45% at the room temperature, 300 and 600 °C heating temperature, respectively. This is because with increase in cutting speed the cutting zone temperature was

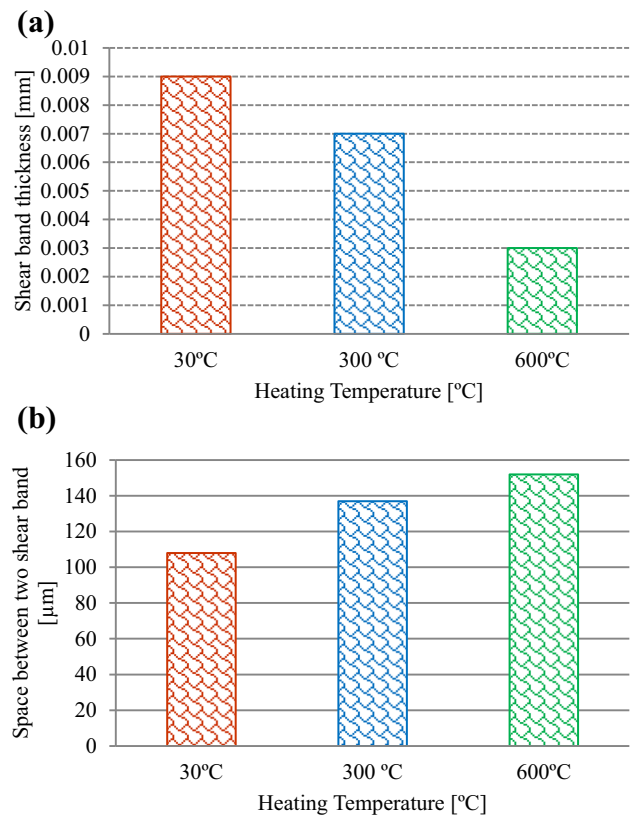


Fig. 12 Influence of heating on shear band thickness (a) and space between shear band (b)

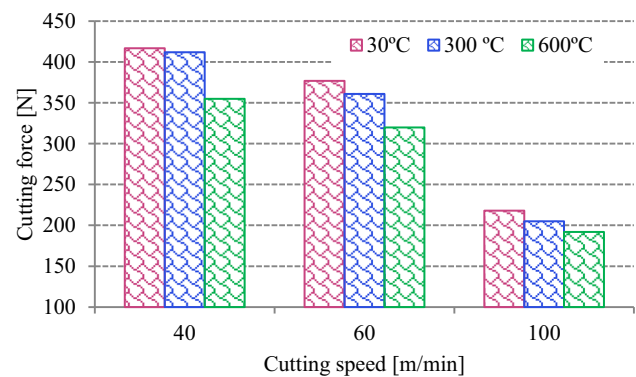


Fig. 13 Effect of heating on cutting force at different cutting speed

also increased which again reduced heat generation due to plastic deformation during machining, and hence cutting force decreased as shown in Fig. 13. This type of observation was observed by Thandra and Choudhury (2010) in machining of high-strength material.

4 Conclusion

With the effect of heating on shear localization and chip segmentation, the following conclusions may be drawn:

- At room temperature, the mechanism for chip segment formation is a combination of plastic strain and fracture, whereas for heating conditions (600 °C) is the plastic strain. In both room and heating conditions, mode II type fracture occurs, but the fracture at heating temperature was found less compared to room temperature;
- Due to heating, the material strength decreased, so cutting force decreases which represents that the segmentation ratio and frequency of serration were decreased with the increase in heating temperature;
- Equivalent chip thickness decreased with the increased heating temperature, but it increases with increase in cutting speed;
- Shear plane length and saw-tooth spacing decreased with the increase in heating temperature compared to room temperature;
- Shear band thickness decreased with heating, but shear band spacing increased with heating compared to room temperature;
- The cutting force decreased with increase in heating temperature and increase in cutting speed again reduced the cutting speed due to reduction in heat generation as a result of plastic deformation during machining.

References

- Amin AKMN, Sulaiman SA, Arif MD (2012) Development of mathematical model for chip serration frequency in turning of stainless steel 304 using RSM. *Adv Mater Process Technol Pts 1–3*(217–219):2206–2209. <https://doi.org/10.4028/www.scientific.net/AMM.217-219.2206>
- Atlati S, Haddag B, Nouari M, Zenasni M (2011) Analysis of a new segmentation intensity ratio SIR to characterize the chip segmentation process in machining ductile metals. *Int J Mach Tools Manuf* 51:687–700. <https://doi.org/10.1016/j.ijmactools.2011.05.007>
- Baili M, Wagner V, Dessein G (2011) An experimental investigation of hot machining with induction to improve Ti-5553 machinability. *Appl Mech Mater* 62:67–76. <https://doi.org/10.4028/www.scientific.net/AMM.62.67>
- Bäker M (2005) Finite element investigation of the flow stress dependence of chip formation. *J Mater Process Technol* 167:1–13. <https://doi.org/10.1016/j.jmatprotec.2004.09.076>
- Calamaz M, Coupard D, Girod F (2008) A new material model for 2D numerical simulation of serrated chip formation when machining titanium alloy Ti–6Al–4V. *Int J Mach Tools Manuf* 48:275–288. <https://doi.org/10.1016/j.ijmactools.2007.10.014>
- Cotterell M, Byrne G (2008) Dynamics of chip formation during orthogonal cutting of titanium alloy Ti–6Al–4V. *CIRP Ann Manuf Technol* 57:93–96. <https://doi.org/10.1016/j.cirp.2008.03.007>
- Ezugwu EO, Bonney J, Yamane Y (2003) An overview of the machinability of aeroengine alloys. *J Mater Process Technol* 134:233–253. [https://doi.org/10.1016/S0924-0136\(02\)01042-7](https://doi.org/10.1016/S0924-0136(02)01042-7)
- Germain G, Lebrun JL, Braham-Bouchnak T et al (2008) Laser-assisted machining of Inconel 718 with carbide and ceramic inserts. *Int J Mater Form* 1:523–526. <https://doi.org/10.1007/s12289-008-0213-y>
- Ginta, TL, Amin AKMN, Lajis MA (2009) Improved tool life in end milling Ti–6Al–4V through workpiece preheating. *Eur J Sci Res* 27(3):384–391. ISSN: 1450-216X
- Ginta TL, Amin AKMN (2013) Thermally-assisted end milling of titanium alloy Ti–6Al–4V using induction heating. *Int J Mach Mach Mater* 14:194–212. <https://doi.org/10.1504/IJMMM.2013.055737>
- Hinds BK, De Almeida SM (1981) Plasma arc heating for hot machining. *Int J Mach Tool Des Res* 21:143–152. [https://doi.org/10.1016/0020-7357\(81\)90005-6](https://doi.org/10.1016/0020-7357(81)90005-6)
- Hua J, Shivpuri R (2004) Prediction of chip morphology and segmentation during the machining of titanium alloys. *J Mater Process Technol* 150:124–133. <https://doi.org/10.1016/j.jmatprotec.2004.01.028>
- Joshi S, Tewari A, Joshi S (2014) Influence of preheating on chip segmentation and microstructure in orthogonal machining of Ti–6Al–4V. *J Manuf Sci Eng* 135:1–11. <https://doi.org/10.1115/1.4025741>
- Joshi S, Tewari A, Joshi SS (2015) Microstructural characterization of chip segmentation under different machining environments in orthogonal machining of Ti–6Al–4V. *J Eng Mater Technol* 137:11005. <https://doi.org/10.1115/1.4028841>
- Kittagawa T, Maekawa K (1990) Plasma hot machining for new engineering materials. *Wear* 139:251–267. [https://doi.org/10.1016/0043-1648\(90\)90049-G](https://doi.org/10.1016/0043-1648(90)90049-G)
- Komanduri R, Brown RH (1981) On the mechanics of chip segmentation in machining. *J Eng Ind* 103:33. <https://doi.org/10.1115/1.3184458>
- Leshock CE, Kim JN, Shin YC (2001) Plasma enhanced machining of Inconel 718: modeling of workpiece temperature with plasma heating and experimental results. *Int J Mach Tools Manuf* 41:877–897. [https://doi.org/10.1016/S0890-6955\(00\)00106-1](https://doi.org/10.1016/S0890-6955(00)00106-1)
- López de Lacalle LN, Perez J, Llorente JI, Sanchez JA (2000) Advanced cutting conditions for the milling of aeronautical alloys. *J Mater Process Technol* 100(1–3):1–11
- López de Lacalle LN, Sánchez JA, Lamikiz A, Celaya A (2016) Plasma assisted milling of heat-resistant superalloys. *ASME J Manuf Sci Eng* 126:274–285. <https://doi.org/10.1115/1.1644548>
- Lorentzon J, Jarvstrat N, Josefson BL (2009) Modelling chip formation of alloy 718. *J Mater Process Technol* 209:4645–4653. <https://doi.org/10.1016/j.jmatprotec.2008.11.029>
- Maity KP, Swain PK (2008) An experimental investigation of hot-machining to predict tool life. *J Mater Process Technol* 198:344–349. <https://doi.org/10.1016/j.jmatprotec.2007.07.018>
- Norazlan MW, Mohid Z, Rahim EA (2013) Laser assisted machining of titanium alloys. *Mater Sci Forum* 763:91–106. <https://doi.org/10.4028/www.scientific.net/MSF.763.91>
- Novak JW, Shin YC, Incropera FP (1997) Assessment of plasma enhanced machining for improved machinability of Inconel 718. *J Manuf Sci Eng* 119:125. <https://doi.org/10.1115/1.2836550>
- Özler L, Özel C (2001) Theoretical and experimental determination of tool life in hot machining of austenitic manganese steel. *Int J Mach Tools Manuf* 41:163–172. [https://doi.org/10.1016/S0890-6955\(00\)00077-8](https://doi.org/10.1016/S0890-6955(00)00077-8)
- Parida AK, Maity KP (2016a) Finite element method and experimental investigation of hot turning of Inconel 718. *Adv Eng Forum* 16:24–32. <https://doi.org/10.4028/www.scientific.net/AEF.16.24>
- Parida AK, Maity KP (2016b) An experimental investigation to optimize multi-response characteristics of Ni-hard material using

- hot machining. *Adv Eng Forum* 16:16–23. <https://doi.org/10.4028/www.scientific.net/AEF.16.16>
- Parida AK, Maity KP (2016c) Optimization in hot turning of nickel based alloy using desirability function analysis. *Int J Eng Res Afr* 24:64–70. <https://doi.org/10.4028/www.scientific.net/JERA.24.64>
- Parida AK, Maity KP (2016d) Engineering science and technology, an international journal effect of nose radius on forces, and process parameters in hot machining of Inconel 718 using finite element analysis. *Eng Sci Technol Int J*. <https://doi.org/10.1016/j.jestch.2016.10.006>
- Polvorosa R, Suárez A, Lopez de Lacalle LN, Cerrillo I, Wretland A, Veiga F (2017) Tool wear on nickel alloys with different coolant pressures: comparison of alloy 718 and Waspaloy. *J Manuf Process* 26:44–56. <https://doi.org/10.1016/j.jmapro.2017.01.012>
- Sun S, Brandt M, Dargusch MS (2010) Thermally enhanced machining of hard-to-machine materials: a review. *Int J Mach Tools Manuf* 50:663–680. <https://doi.org/10.1016/j.ijmachtools.2010.04.008>
- Thandra SK, Choudhury SK (2010) Effect of cutting parameters on cutting force, surface finish and tool wear in hot machining. *Int J Mach Mach Mater* 7:278. <https://doi.org/10.1504/IJMMM.2010.033070>
- Wang C, Xie Y, Zheng L (2014) Research on the chip formation mechanism during the high-speed milling of hardened steel. *Int J Mach Tools Manuf* 79:31–48. <https://doi.org/10.1016/j.ijmachtools.2014.01.002>
- Xue Q, Meyers MA, Nesterenko VF (2002) Self-organization of shear bands in titanium and Ti–6Al–4V alloy. *Acta Mater* 50:575–596. [https://doi.org/10.1016/S1359-6454\(01\)00356-1](https://doi.org/10.1016/S1359-6454(01)00356-1)
- Yilbas BS, Akhtar SS, Karatas C (2010) Laser surface treatment of Inconel 718 alloy: thermal stress analysis. *Opt Lasers Eng* 48:740–749. <https://doi.org/10.1016/j.optlaseng.2010.03.012>